Contributed paper

OPTO-ELECTRONICS REVIEW **8**(2), 153–159 (2000)

Biconical fused taper – a universal fibre devices technology

K. JĘDRZEJEWSKI*

Institute of Electronic Systems, Warsaw University of Technology
15/19 Nowowiejska Str., 00-665 Warsaw, Poland

The development of optical fibres has resulted in a range of components fully compatible to the optical network. The number of such devices is steadily growing. Fibre connectors, couplers, multi- and demultiplexers, filters, polarisers, sensors, amplifiers, lasers and superluminescent diodes made of cylindrical fibres are widely used in optical telecommunication and sensor networks. Only the light detectors cannot be found in the fibre form yet. The revue and some recent applications are given for biconical fused fibre taper techniques. The variety of experimental solutions of taper designs developed in the Institute of Electronic Systems (ISE), Warsaw University of Technology is presented.

Keywords: optical fibre, biconical fused fibre taper techniques.

1. Introduction

The most successful practical application of single–mode biconical tapering technique has been achieved in the design of low-loss fused directional coupler. By heating, stretching and tapering of two fibres a fused structure was developed in which power coupling from one to the other fibre is possible. These processes can be proceeded in many ways and the wavelength dependence of coupling can be intentionally decreased or increased. Directional couplers, WDMs and filters are easily made by this method. These components are widely used in long-distance telecommunication networks, LAN's, fever common are the applications in optical metrology especially as the sensing devices.

The easiest form to analyse the device is the single fibre taper or 2×2 coupler where the energy transfer is achieved by the side coupling of the fundamental modes in two fibres aligned and bonded together. Properly made tapered devices are characterised by low excess losses, much below 1 dB. It is well known from experiments that it is quite easy to taper thermally a single fibre, i.e., locally lower the diameter more then 40 times without significant losses (< 0.1 dB).

2. Theoretical background

Initially the field is guided by, and substantially confined to, the core. For the normalised frequency V = 2.4 and the weakly guided structure 86% of the energy is transmitted inside the core. As the fibre is down tapered the fundamental mode in the core-clad system spreads gradually out (for V = 1 only 26% of the signal stays inside the core in the weakly guided fibres) until it reaches the outer surface of the cladding. At the cladding/air interface the weakly guided mode (the V value locally decreases during tapering) is progressively transferred to the strong guided behaviour in the glass/air structure and the fibre tends to propagate as multimode. The power coupled to the higher order modes is undesirable and can produce significant losses of the transmitted signal. The persuasive adiabaticity criterion [1] has been derived for keeping the funnel angle sufficiently small to avoid the energy transfer from the fundamental mode LP_{01} to the higher order modes of the same symmetry.

The field distribution for the fundamental mode is close to the Gaussian mode for the step–index fibre and V = 2.4. For the smaller V, as the core diameter decreases the field spreads out and its spot size increases as

$$\frac{\tau}{a} = 0.65 + \frac{1.619}{V^{3/2}} + \frac{2.879}{V^6}. \tag{1}$$

It is valid within the accuracy of 1%, where a is the core diameter, τ is the mode field diameter.

The beam divergence is a balance between spreading due to diffraction of the modal field caused by the finite core diameter

$$\theta_d = \frac{2\lambda}{\pi n_1 \tau} \tag{2}$$

(where τ is the Gaussian mode field diameter in the fibre waist, n_1 is the refractive index of the core glass) and mode concentration due to the differences between core and cladding refraction indices θ_c. For the weakly guided structures

$$\theta_c = (2\Delta)^{1/2} \tag{3}$$

Δ is the relative refractive index difference.

*e-mail: kpj@ise.pw.edu.pl

The spread of the modal field will be a minimum when these two effects are comparable [2]. For the step-index fibre it happens when V ≈ 2 for core-clad structure. Further tapering increases the spot size diameter due of diffraction until the glass-air interaction as the outer cladding. The minimum is again expected for the new V ≈ 2 calculated for the glass-air structure. During further tapering spot size increases monotonically as the field spreads out into the air.

If the tapered fibre has an identically processed neighbour, the fields of both fibres can interact and the power can be transferred from one to other. The quantity of this interaction depends on many variables as fibre NA (core and cladding refractive indexes), core radii, degree of the taper, distances between the cores, the coupling lengths and wavelength.

The coupler analysis can be performed in two different approaches. In the first Maxwell's equations it can be solved for the coupler system as a whole. This is difficult because of the different cross-sectional shapes along the taper and the field distortion from symmetry and circularity. In the second approach the field of the two waveguide system is a combination of two fields of each individual fibre along the taper.

The coupling strength is dependent on the fields overlap of both tapers. The power propagated in each fibre along the z-axis (fibre axis) is given $|a_1(z)|^2$ by and $|a_2(z)|^2$; $a_1(z)$ and $a_2(z)$ are the length dependent mode amplitude coefficients and satisfy equations

$$\frac{da_1(z)}{dz} = -iC_{21}e^{i\Delta\beta z}a_2(z)$$

and

$$\frac{da_2(z)}{dz} = -iC_{12}e^{i\Delta\beta z}a_1(z), \tag{4}$$

where $\Delta\beta = \beta_1 - \beta_2$, β_1 and β_2 are the propagation constants of two fibres, C_{12} and C_{21} are the coupling coefficients.

When the fibres are identical, i.e., $\beta_1 = \beta_2$, then $C_{12} = C_{21} = C_0$ and the power propagated along both fibres is given by

$$P_1(z) = |a_1(z)|^2 = P_0 \sin^2(C_0 z)$$

and

$$P_2(z) = |a_1(z)|^2 = P_0 \cos^2(C_0 z). \tag{5}$$

The complete energy transfer from one fibre to the other occurs at distances L, 2L, 3L, ..., where

$$L = \frac{p}{2C_0}. \tag{6}$$

For a strongly fused coupler modelled by a rectangular waveguide in the neck section the coupling coefficient can be expressed as [3]

$$C_0 = 3\pi\lambda\left[32n_2a^2(1+\frac{1}{V})^{-1}\right], \tag{7}$$

with the local normalised frequency defined as

$$V = ak(n_2^2 + n_3^2)^{1/2} \tag{8}$$

where a is the dimension of the neck rectangle, n_2, n_3 are the refractive indices of cladding and the surrounding medium, λ is the wavelength in the vacuum, $k = 2\pi/\lambda$.

From this equation the periodical changes with λ is revealed. The oscillation period $\Delta\lambda$ varies because of C_0 and V dependence of λ for a coupler.

3. Experimental set-up

In the early experiments the gravitational pull was preferred. The plastic acrylate fibre jackets were removed to expose the glass and the fibres were twisted together. The glass was heated to its softening point by a miniature oxybutane flame. The heater was build as a line of small (0.6 mm diameter) holes and total length of 5–15 mm. The gas flow and air/gas composition was carefully adjusted by precisely designed needle valves. The fibres were slowly pulled down after reaching the desired temperature. The speed of the process was easily controlled by changing the distance between fibres and the flame. The main disadvantage of the system was the asymmetry of upper and bottom taper especially when small weights were used for the pulling sensitivity adjustment. The adiabaticity criterion for the upper taper could be exceeded causing accidentally unexpected excess losses of the device.

In the horizontal rig the stepping motor was used to transport linearly and horizontally a single hole burner along the fibres (Fig. 1). The scan distance can be set from 0 to 24 mm in 0.3 mm steps. The stepping motor movement was controlled via the PC computer. The scan speed and speed variations of the flame, scan length and the heating time in the desired time moments and duration can be easily programmed in this system. The fibres were pulled symmetrically via the DC motor. The pull speed was controlled by changing the motor voltage supply. The taper angles can be programmed and tailored in this system.

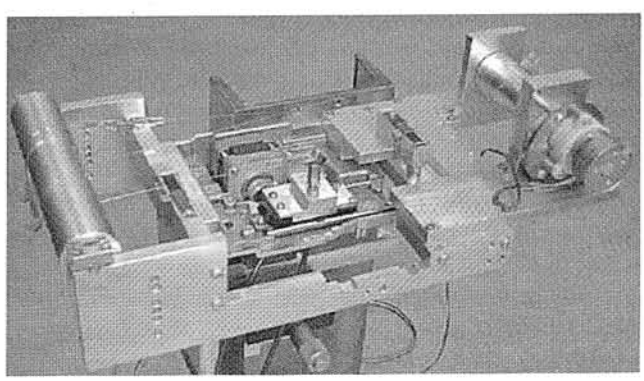

Fig. 1. Horizontal tapering system. The movable programmable stepping motor driven heater can be seen in the centre of photograph, DC pull motor is on the right, simultaneous and equal pull force is achieved via synchronised cylinders located on both sides of the picture.

Both tapers were symmetrical in the horizontal arrangement. There was no problem with the adiabaticity and the unexpected losses. The measured taper angles were much below the limit and the excess losses were typically below 0.1 dB. The couplers were better environmentally stable (with temperature). The total coupler length can be lowered to 15–30 mm together with the case. A typical taper shape is presented in Fig. 2.

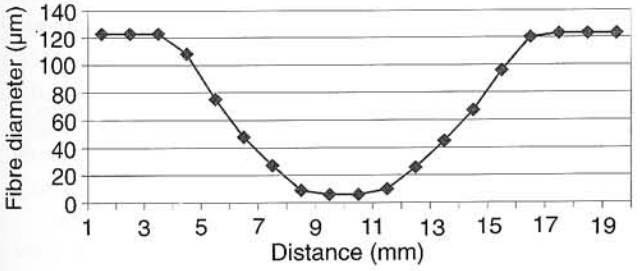

Fig. 2. Diameter changes along a tapered fibre, similar to the coupler of Fig. 5; horizontally pulled, burner scanning distance 3 mm, pull speed 10 mm/min, total elongation length 14 mm.

4. BFT fibre devices

4.1. Beam expander

To exploit the tapered single-mode fibre as a practical beam expander, it was necessary to strengthen the taper along its length for better stiffness and handling [4]. The capillary jacket protects also the expanded beam from external refractive index change and the damage. The Vycor capillary sleeve of about 350/270 μm external to internal diameter was placed around the fibre. The capillary was then collapsed uniformly around the fibre before tapering using a symmetrical heat distribution provided by a miniature graphite furnace with argon atmosphere. The simple oxybutane flame did not provide the necessary symmetry in collapse and gave rise to higher order modes couplings during tapering with resultant losses.

The combined fibre and capillary were then tapered to the neck diameter of about 40 μm. This diameter was still appropriate for sufficient handling and cleaving. Vycor has a slightly lower refractive index then silica, of about 0.004. The formed expanded cladding mode is now guided by the boundary of the fibre cladding and Vycor.

The complete fibre–capillary structure tapered in the graphite furnace allows good control and slow tapering. Excess losses were kept below 0.7% for taper ratios of typically 4:1. The near-field spot-size of the fundamental mode was measured as it evolved along such taper. The measurements of the mode field diameter were made by progressively cleaving back the tapered structure. The spot size increased in these experiments from 2,6 μm to 6–7 μm in the fibre neck. Experimental data is in a very good agreement to the calculations [2]. The step-index silica fibre was used in these experiments with the cut-off of 600 nm. The visible red He-Ne laser was the light source in these experiments. The transmission of light was controlled during the elongation process.

Theoretically a longitudinal gap (separation) between two single–mode fibres results in a transmission loss of 10lgT [5], where

$$T = \frac{4z^2 + 1}{(2z^2 + 1)^2 + z^2} \tag{9}$$

$z = D/(n_1 k \tau_2)$, $k = 2\pi/\lambda$, D is the separation distance, τ is the local mode field diameter, n_1 is the refractive index of the core.

Figure 3 shows plots of the transmission coefficients (both as given by equation and as measured) for a standard λ_c = 600 nm single-mode step-index fibre with the spot–size of 2.6 μm for the tapered and not tapered structure. The connection was immersed in an index matching medium. The 3-dB losses value is achieved at the distance of 100 μm. It can be seen from the equation that the spot-size for a given loss increases as the square of the spot size. A moderate increase in the spot size to 6 μm will result in a big gap increase of 600 μm for 3-dB loss. The beam divergence changes were seen at the cleaved taper forming a kind of taper lens.

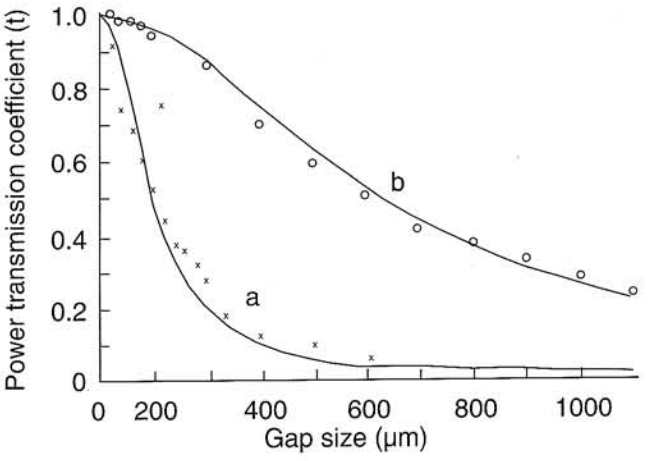

Fig. 3. Power transmission (relative values) as a function of fibres ends separation (gap size) for: (a) non tapered 2.6 μm spot size fibre and (b) 6.0 μm spot size tapered fibre (in immersion fluid).

Low loss expanded beam fibre tapers may be considered as the rugged, fibre compatible alternatives to lens beam expanders in connectors, pigtailed semiconductor lasers and power splitters. Carefully prepared tapers allow us to minimise the connection losses for different spot size SM fibres connections [6], e.g., with non-silica fibre amplifiers. Other in-line fibre devices prepared in this form are acoustooptic modulators, liquid crystal choppers, sensors inserted directly into the gap.

4.2. Biconically fused couplers

4.2.1. Typical coupler characteristics

The technological problem to simultaneously fuse and taper two fibres together is far more complex. Initially the two identical fibres are twisted together to achieve good contact of their carefully prepared and cleaned surfaces. It is advisory and convenient to excite one of the input ports and monitor the output signals at all outputs during elongation process. Fig. 4 shows a plot of the output powers versus elongation of the input fibre. For tapers of lengths indicated 1, 2, and 3 the input power is divided equally between the output ports (3 dB coupler). Any other desirable coupling ratio can be obtained carefully controlling the elongation process. The periodicity predicted from equations (5) should be maintained. In a practical real coupler the decrease of the waist diameter introduces changes in the coupling ratio values C_0. The $\cos^2$ and $\sin^2$ variation period decreases with elongation. The same behaviour is observed in the spectral response as C_0 is dependent on λ. An example of the spectral characteristic of a coupler made in our laboratory is given in Fig. 5. The coupler was made as 3-dB coupler for 1310 nm, for the first output power equalisation (point 1 of Fig. 4). The split ratio SR spectral changes are typically 0.12–0.15%/nm for the first 3 dB division of the signal along the fibre during elongation (simplest commercially available couplers).

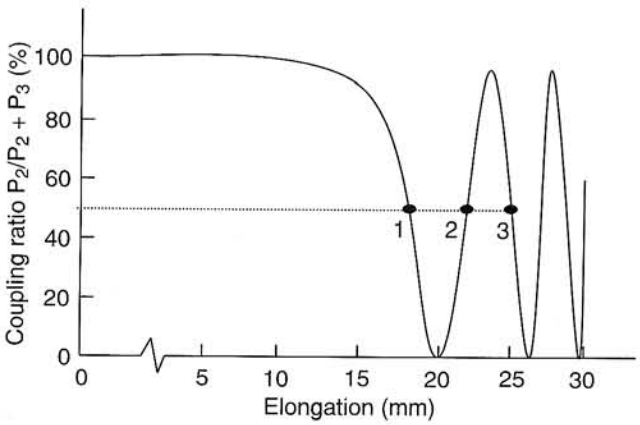

Fig. 4. Coupling ratio vs. elongation during pulling for a typical 2×2 single-mode coupler; pulled and controlled at 1310 nm.

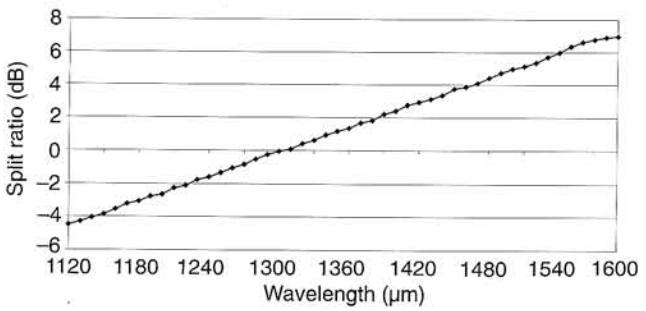

Fig. 5. Split ratio spectral response of a 3 dB coupler designed for 1310 nm made by the horizontal technique (sample no. 185H), measured excess losses 0.07 dB.

4.2.2. Broadband couplers

The tapered biconical directional couplers are typically narrowband devices. Two fibres with different core diameters can be used for wideband flat spectral response of a 2×2 coupler. For the couplers made of different fibres where $\Delta\beta \neq 0$, the total energy transfer is not possible [7]

$$P_1(z) = \left[1 + \left(\frac{\Delta\beta}{2C}\right)^2\right]^{-1/2} \times \sin^2\left\{\left[C^2 + \left(\frac{\Delta\beta}{2}\right)^2\right]^{1/2}\right\}$$

and

$$P_2(z) = 1 - P_1(z) \tag{10}$$

The wavelength flattened broadband couplers can be made using fibres with the different β [8]. The core diameter difference should be very small, about 1.5% only.

We propose chemical polishing of the outer surface as the alternative technique of decreasing the fibre outer diameter as the less expensive way then to employ two different fibres with slightly different core sizes from a commercial producer [9]. Careful chemical polishing treatment with controlled temperature in an experimentally derived solution of HF and H_2SO_4 in water was developed to keep very smooth surface of the fibre during polishing. The glass surface was checked out by the optical microscope after drying. The polishing time was very short, determined experimentally of 3–4 min approximately.

Using partially the same technology as for conventional couplers, the broadband couplers can be made. We produced the broadband couplers with excess losses of 0.1–0.5 dB and with the pigtails fully compatible to the fibres in the network. The spectral changes of the split ratio were lowered tenfold to 0,015%/nm in comparison to the typical coupler. The spectral response of such coupler is presented in Fig. 6. It shows that the 3 dB coupler with 0.3 dB losses (controlled at 1310 nm) was made with the

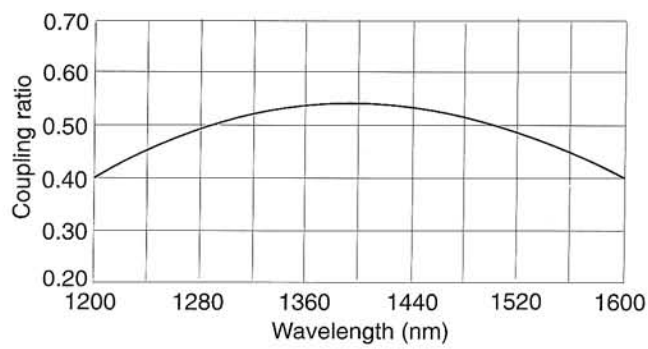

Fig. 6. Spectral dependence of the coupling ratio for the broadband coupler designed as 3 dB coupler for 1310 and 1520 nm.

split ratio tolerances of only 5% in the wavelength region 1240–1550 nm. The "wavelength insensitive coupler" made of chemically prepolished fibres was realised.

4.2.3. Multiplexers and filters

The ideal situation for making a wavelength division multiplexer/demultiplexer (WDM) is to pull the coupler up to the point where the coupling ratio is 0% for one wavelength (eg., 1310 nm) and 100% for the other (e.g., 1550 nm). We monitor the signal at one wavelength only. The second wavelength is adjusted experimentally for consequent minima and maxima of Fig. 4. Figure 7 shows the experimental data of 1310/1550nm multi/demultiplexer. The isolation of 30 dB for 20 nm bandwidth was measured.

In practice, it is difficult to obtain an ideal coupling and very high isolation between the channels. The future of such devices is less attractive in comparison to the DWDM systems incorporating the Bragg gratings but the presented solution is still much cheaper for two distant wavelengths operation. The 1480/1550 multiplexer for EDFA pumping was also made of the same fibre with 20–dB isolation. Further tapering to achieve lower wavelength gap between two signals introduces the undesired polarisation influence clearly visible as an envelope in the measured spectra.

When tapering the depressed cladding fibres or abruptly tapering the matched clad fibres the adiabaticity criterion is not satisfied. The oscillatory character of the output signal is expected and a fibre filter can be made in an uncontrollable way. Tapered multiplexer is in fact also a broad bandpass filter. The taper length should be far more extended and the waist diameter lowered to increase the spectral oscillations and decrease the filter bandwidth. The minimum FWHM value achieved in the experiments was 9 nm. In the case of two cascaded couplers only the side lobes could be lowered and the isolation increased. The addition of further couplers is increasingly time consuming. The low loss and fibre compatibility of such all-fibre filter is the advantage over bulk interference device. The Bragg grating filters technology is a much better solution for such applications now.

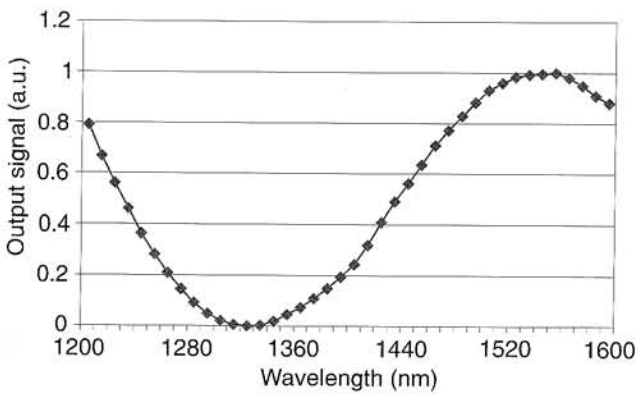

Fig. 7. Spectral response of 1310/1550 tapered multiplexer; excess loss 0.2 dB.

4.3. A taper in an acoustic field

Fibre bends introduce additional losses by coupling the guided signal into other guided or radiation modes. The micro-bend fibre optic sensor is a typical example in which this behaviour was practically applied [10]. The periodic structure of microbends introduces the optical path differences and local refractive index variations caused by strain via the elastooptic effect. The couplings from the fundamental mode LP_{01} to the higher order modes, e.g., LP_{11} are possible in the same manner as it is in the long period diffraction gratings formed in the germanium doped fibre cores by the ultraviolet radiation. The part of energy propagated in LP_{11} mode not necessarily will be taken back to the fundamental mode after passing the bending region causing losses now. The maximum coupling between the modes is possible when the perturbation period and the beatlength between LP_{01} and LP_{11} modes are synchronous [11].

The acoustooptic transducer can be applied as the travelling acoustic flexural waves generator. The coupled light is frequency Doppler shifted which is equal to the acoustic frequency of the transducer [12].

The overlap between optical and acoustic waves is normally very poor and acoustic wave power supply need to be high. To reduce it a PZT disc was attached to the fibre by the metal concentrator. To increase additionally the sensitivity the effect was observed in a typical fibre taper where the mode transition is more effective. Much lover acoustic power is needed now to see this behaviour [13].

The wavelength of the implemented flexural acoustic waves travelling along the fibre Λ is

$$\Lambda = \sqrt{\frac{\pi R c_{ext}}{f}}, \tag{11}$$

where R is the fibre waist radius, c_{ext} is the acoustic wave speed in silica, f is the acoustic wave frequency.

The beatlength L_B between the fundamental and the next LP_{11} mode in the singlemode fibre is

$$L_B = \frac{8\pi^2 R^2 n}{(j_{11}^2 - j_{01}^2)\lambda}, \tag{12}$$

where n is the glass refractive index, j_{11} and j_{01} are the Bessel function first roots of the first and zero order 3.832 and 2.405, respectively, λ is the light wavelength.

When

$$\Lambda = L_B, \tag{13}$$

resonance condition between optical and acoustical waves is satisfied and energy transfer between LP_{01} and LP_{11} modes is possible. The LP_{11} mode is not propagated in a single mode fibre. The energy radiated into the cladding is quickly attenuated in the acrylate coating with the higher refractive index value then in the glass.

We optimised the best operation frequency experimentally. The transmitted light wavelength was 1310 nm. The spectral characteristics show some oscillations considerably decreasing the bandwith. We assume the small birefringence responsible for such behaviour, which is introduced by the acoustic waves excited in one plane of the fibre only. The PZT transducer PFD PP9 (Cerad PL) was glued to the fibre very close to the taper region via the aluminium cone. Such a double conical structure minimises the energy needed for energy transfer between the modes in a taper of the diameter approximately 10 μm in the waist. Our vibrometer resolution was not sufficient for the acoustic amplitude measurements in the taper region of the device. The final data is given in Fig. 8. With the increase in the signal generator drive voltage the acoustic amplitude increases the coupling between the modes and the signal at the output of the fibre decreases.

The fibre compatible attenuator made of typical telecommunication fibre was realised [14]. The tuning range 0–13 dB was easily regulated by the low power and low frequency typical electronic sinewave generator (Fig. 8). The excess losses of the taper were very low typically in the range 0.1–0.3 dB. By switching the acoustic power on and off, the electronic light chopper can be an easily made replacing incompatible to fibre mechanical devices.

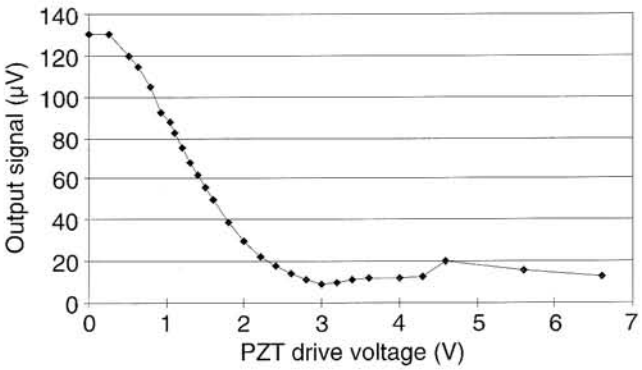

Fig. 8. The output signal changes with the generator drive voltage U_o (f = 589 kHz, λ = 1310 nm).

4.4. Couplers for metrology

The environmental stability is the fundamental property for real, field applications of a coupler. The thermal stability is of greatest importance in most cases. The reason is a very low thermal expansion coefficient of silica (α = 5.10–7 1/°C). The invar tube (α = 15.10–7 1/°C) is the only material to match closely the thermal expansion of glass. The silica substrates are used to avoid the thermal expansion influence.

The couplers prepared at ISE were packed into a very unsuitable aluminium case with a very high expansion coefficient of α = 230.10–7 1/°C and fixed by a very soft silicone rubber. Even for such hostile conditions, the coupling ratio changes did not exceed 1% in the temperature range of –15 ÷ +70°C for the horizontally prepared couplers [15].

On the other side the same tapered coupler bonded strongly with the aluminium case by the epoxy resin shows significant coupling ratio changes. The coupler was packed in the temperature 20°C. There is no evidence of changes if the fibres are strained (> 20°C). It happens only when the fibres are bent (Fig. 9). Similar curves were obtained for mechanical displacement of one of the coupler ends.

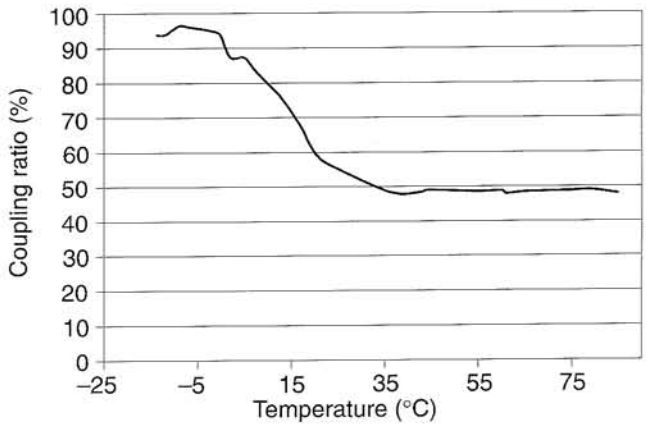

Fig. 9. Changes of the coupling ratio with temperature for a coupler strongly bonded to the case.

If the coupler is primarily bent before applying the resin, a sensor can be made for much wider temperature range (Fig. 10) [16]. The temperature dependent changes vary monotonically with temperature. The temperature range was limited to –15 ÷ +100°C by the measurement possibilities. The differential signal from the coupler outputs doubles the measurement sensitivity. In the computer data acquisition, this slightly nonlinear curve can be easily linearised. The temperature range can be varied by controllable fibre bends. It is quite easily achievable in the horizontal pulling system.

More applications of a coupler can be expected for sensing application. The field expanded to the glass/air interface is sensitive on refractive index changes or spectral

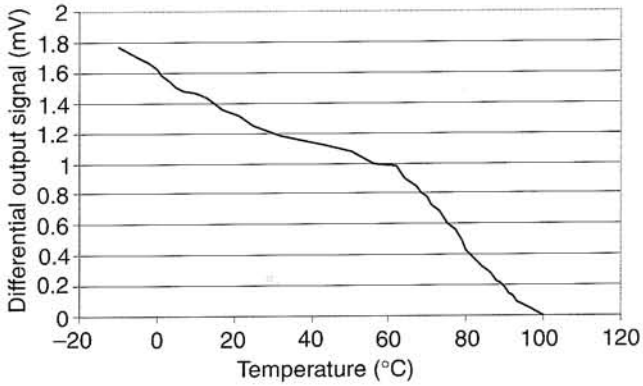

Fig. 10. Differential signal changes from both coupler outputs vs. temperature.

absorption of the surrounding medium. The drastic change of their refractive index can lead to switching mode between the output arms.

5. Conclusions

The already old fashioned technique for making tapers introduced 15 years ago is still one of the best for making low loss, fully compatible devices with the fibre network. Some new applications can be found as sensors or switching devices with the acoustic waves assistance. In the case of a Bragg DWDM two couplers are also necessary for making an interferometer for each wavelength-dividing element. The planar technology will be advantageous in the future, but still the losses on the cylindrical/planar interface are very high.

Acknowledgments

Author thanks the colleagues from the ORC University of Southampton and the ISE Warsaw University of Technology for help and encouragement.

References

1. W.J. Stewart and J.D. Love, "Design limitation on tapers and couplers in single-mode-fibres", *IOOC/ECOC Tech. Digest* **1**, 559–562 (1985).
2. J.D. Love, "Spot size, adiabaticity and diffraction in tapered fibres", *Electron. Lett.* **23**, 993–994 (1987).
3. F.P. Payne, C.D. Hussey, and M.S. Yataki, "Modelling fused single-mode-fibre couplers", *Electron. Lett.* **21**, 461–462 (1985).
4. K.P. Jędrzejewski, F. Martinez, J.D. Minelly, C.D. Hussey, and F.P. Payne, "Tapered-beam expander for single-mode optical-fibre gap devices", *Electron. Lett.* **22**, 105–106 (1986).
5. Y. Tamura, H. Maeda, S. Shiki, and B. Yokoyama, "Single-mode fibre WDM in the 1.2/1.3 micron wavelength region", *IOOC/ECOC Tech. Digest* **1**, 579 (1985).
6. J.D. Minelly, "Field access techniques for single-mode fibres", PhD Theses, University of Southampton, 1989.
7. M.J.F. Digonnet and B.Y. Kim, "Fiber optic components", in *Optical Fiber Sensors*, edited by J. Dakin and B. Culshaw, Artech House, Boston and London, 1988.
8. V.J. Tekippe, "Passive fibre optic components made by the fused biconical taper process", V Symp. on *Optical Fibres and Their Applications*, Warsaw, Poland, **3**, 119–147 (1989).
9. K. Jędrzejewski and A. Kosiński, "Wide–band tapered directional coupler", *Proc. SPIE* **3189**, 130–132 (1997).
10. J.N. Fields and J.H. Cole, "Fibre optic microbend acoustic sensor", *Appl. Opt.* **19**, 3265 (1980).
11. H.F. Taylor, "Bending effects in optical fibres", *J. Lightwave Technol.* **LT-2**, 617–628 (1984).
12. T.A. Birks, P.St.J. Russell, and D.O. Culverhouse, "The acousto-optic effect in single-mode fibre tapers and couplers", *J. Lightwave Technol.* **14**, 2519–2529 (1996).
13. T.A. Birks, P.St.J. Russell, and C.N. Pannell, "Low power acousto–optic device based on tapered single–mode fibre", *IEEE Photonics Technol. Lett.* **6**, 725–727 (1994).
14. K. Jędrzejewski, M. Franczyk, and A. Leszczyński, "Acousto-optically tuned single-mode in-line fibre attenuator", *Proc. SPIE* **3731**,103–106 (1999).
15. K. Jędrzejewski and P. Wieczorek, "Temperature stability of fused biconical couplers", *Telecom Symposium KST'99*, 8–10 September 1999 Bydgoszcz, **A_8.12**, 401–405 (1999) (in Polish).
16. P. Wieczorek and K. Jędrzejewski, "Tapered single-mode coupler as temperature sensor", *7th Conf. on Fibres and Their Applications*, 14–16 October 1999, Krasnobród, **1**, 90–95 (1999) (in Polish).